Computational Study of Sail Performance of a Racing Yacht

P. Izaguirre-Alza[1], R. Zamora-Rodríguez[1], L. Pérez-Rojas[1]

[1] Model Basin research Group (CEHINAV[1])
Naval Architecture Department (ETSIN)
Technical University of Madrid (UPM)

Abstract

It is important to understand flow characteristics and performance of sails for both sailors and designers who want to have an efficient thrust of yacht. In this article, the airflow around yacht sails with imposed final geometry is simulated using a CFD (Computational Fluid Dynamics) code reproducing full scale measurements. The code is a commercial viscous CFD based on Reynolds-averaged Navier-Stokes (RANS) equations. Three sets of sails are considered: two mainsails alone and one set of mainsail with jib and the parameters in study are mainly the lift, drag, center of effort and pressure coefficient over the sails. The results are compared with both experimental data and numerical computations obtained from other studies. It is concluded that there is good agreement between numerical calculations and full scale data, showing the importance of the use of numerical tools.

Resumen

Es importante entender las características del flujo y el comportamiento de las velas tanto para los navegantes como para los diseñadores que quieren tener un empuje eficiente de la embarcación. En este trabajo, se presenta la simulación del flujo de aire alrededor de las velas, con una geometría final impuesta, y con un código CFD reproduciendo las medidas a escala real. El código numérico utilizado es un CFD viscoso basado en las ecuaciones RANS. Se han considerado tres combinaciones de velas: dos mayores y una mayor más génova y los parámetros estudiados principalmente son la sustentación, resistencia, centro vélico y el coeficiente de presión sobre las velas. Se han comparado los resultados obtenidos con datos experimentales y otros datos numéricos procedentes de otros estudios. El estudio concluye que hay una buena concordancia entre los cálculos numéricos y los datos a escala real, mostrando la importancia de la utilización de estas herramientas numéricas.

INDEX: ***Pg.***

[1] http://canal.etsin.upm.es/

1 Introduction

When designing racing yacht sails the main objective is finding the optimal shape to increase the thrust of the boat. For this purpose, two of the most important features that must be analyzed are the aerodynamic forces and moments which can be determined using CFD, theoretical models, experiments carried mainly in wind tunnels and full scale measurements.

Some of the CFD use inviscid methods for the calculation of the flow separation around sails. This approach is computationally efficient but its applicability is limited until separation occurs; which is a far more common phenomenon than was previously believed. Nowadays, viscous CFD codes are promising in this field. This is a numerical model which describes the dynamic of fluids around bodies based on the resolution of the Reynolds Averaged Navier Stokes (RANS) equations. Several applications of RANS have been used to the study of sails. At the beginning, viscous studies were dedicated to the study of the flows around 2D sails and aerodynamic profiles with and without masts ([1], [2], [3], [4]). Later on, it has been possible to obtain reliable results in three-dimensional viscous flow with separated regions ([5], [6], [7], [8]).

One of the advantages of CFD application is that it can provide not only global quantities like sail forces and moments but also detailed flow information useful for the design of a sail system. It is believed that CFD is a cost-effective tool for the performance prediction of a sailing yacht; it can save a lot of efforts in experiments. But these advanced tools have two major drawbacks: the high computational time and the need of continuous validation. Computing time decreases each day as computer power increases and the appearance of multiprocessors in personal computers make this first drawback less important.

The validation of calculated results is very difficult because it requires data such as sail shape, forces acting on the sails and wind conditions, all measured simultaneously. Traditionally, wind tunnels tests have been carried out to determine aerodynamic forces and moments but the results are not very reliable for extrapolation at full scale due to the difficulty of simulating the elasticity of the sail and rigging. In order to measure the sail forces directly, in 1988 a full scale sailing dynamometer boat was built, [9]. The system, named the MIT Sailing Dynamometer, was a 35-foot boat containing an internal frame connected to the hull by six load cells configured to measure all forces and moments acting on the sails. At the same time, the sail shapes were measured and used for the input data of CFD analysis. In 1997 Masuyama and Fukasawa built the sail dynamometer boat Fujin that was similar to the MIT dynamometer. The results using IACC and IMS type sail were reported in different papers such as [10] and [11]. One of the most recent project was initiated in Germany in which the 10-meter full scale sail force dynamometer was named DYNA. It was based on a 33ft IMS cruiser/racer ([8], [12], [13]).

In the present document, some of the sails arrangements from the paper of Masuyama et al. (2007) [11] are simulated using the commercial package ANSYS ICEM CFD with the viscous ANSYS-CFX 10.0. Three-dimensional shape data were used for the input of numerical calculations and now, the results are compared with the reference sail performance information.

2 Notation

C_L → lift coefficient, eq. [1]
C_D → drag coefficient, eq. [1]
C_P → pressure coefficient, eq. [2]
X_{CE} → "X" coordinate of the center of effort of sails
Z_{CE} → "Z" coordinate of the center of effort of sails
L_c → characteristic length (5 m) approximation to jib and mainsail foot
V → inflow wind speed (different in each case), apparent wind speed
P → pressure
P_{abs} → absolute pressure
S → sail area
ρ → air density (1.185 kg/m^3)

$\nabla y \rightarrow$ mesh spacing between the wall and first node away from the wall

$u_\tau \rightarrow$ tangential speed

$\nu \rightarrow$ kinematic viscosity

$$C_D \quad or \quad C_L = \frac{drag \quad or \quad lift}{\frac{1}{2} \cdot \rho \cdot S \cdot V^2} \qquad \text{Equation [1]}$$

$$C_P = \frac{P - P_{abs}}{\frac{1}{2} \cdot \rho \cdot V^2} \qquad \text{Equation [2]}$$

The origin coordinates is located at the aft face of the mast at the deck level as shown in figure 1. When defining the geometry the local reference system is: x-direction from bow to stern, y-direction from port to starboard and z-direction perpendicular to the previous directions and positive upward. In global reference system (for de CFD code) the x-direction is the flow direction, the z-direction is upward and y-direction is perpendicular to the previous and right-handed.

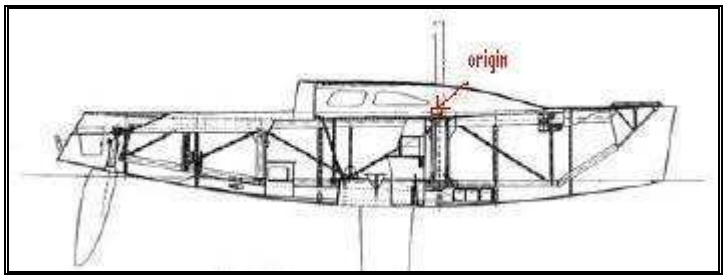

Figure 1: The origin of coordinates

3 Full Scale Testing and Definition of Geometry

As it has been mentioned, in the reference [11], different sail performance and shapes were measured using a sail dynamometer boat Fujin. This boat is a 34-foot boat, in which load cells and cameras were installed to measure the sail forces and shapes simultaneously. The sailing conditions of the boat, such as boat speed, heel angle, wind speed, wind angle and so on, were also measured. The principal dimensions of Fujin are:

- Overall length: 10.35 m
- Waterline length: 8.80 m
- Maximum beam: 3.37 m
- Beam: 2.64 m
- Displacement: 3.86 t

In this paper three cases are going to be analyzed: the main sail in two sailing conditions and the jib + mainsail in another condition. According to of Masuyama et al. [11] these three cases were named: ID 9807172F (mainsail alone), ID 9807172B (mainsail alone) and ID 96092335 (jib + mainsail). The particulars of the jib and the mainsail are:

- Peak height of mainsail: 13.82 m
- Luff length of mainsail: 12.50 m
- Foot length of mainsail: 4.44 m
- Mainsail area: 33.20 m^2

- Peak height of the jib: 10.70 m
- Luff length of the jib: 11.45 m
- Foot length of the jib: 4.89 m
- Jib area: 26.10 m^2

The three sailing upwind conditions are presented in table 1. As it can be seen in the table 2, the shapes of the sails were given by six points in each of the six sections in which sails were divided. Because of the fact that the geometry of the mast was not provided in the reference paper, the study that is presented in this document was undertaken without mast.

	ID 9807172F	**ID 9807172B**	**ID 96092335**
Heel Angle	8.79º	8.72º	14.32º
Apparent Wind Angle	- 30.53º	- 29.88º	- 30.50º
Apparent Wind Speed (V)	7.27 m/s	7.19 m/s	6.81 m/s

Table 1: Sailing conditions

ID 9807172F

%of heit	Mainsail x	Mainsail y	Mainsail z
0 %	0.046	0.000	1.320
	0.934	0.000	1.320
	1.822	0.000	1.320
	2.710	0.000	1.320
	3.598	0.000	1.320
	4.486	0.000	1.320
20 %	0.133	0.000	3.820
	0.869	0.276	3.820
	1.615	0.443	3.820
	2.372	0.492	3.820
	3.138	0.453	3.820
	Without Jib		
40 %	0.221	0.000	6.320
	0.793	0.349	6.320
	1.389	0.569	6.320
	2.010	0.660	6.320
	2.651	0.648	6.320
	3.301	0.590	6.320
60 %	0.308	0.000	8.820
	0.712	0.315	8.820
	1.141	0.549	8.820
	1.607	0.664	8.820
	2.095	0.707	8.820
	2.595	0.712	8.820
80 %	0.396	0.000	11.320
	0.626	0.181	11.320
	0.867	0.338	11.320
	1.126	0.454	11.320
	1.405	0.527	11.320
	1.692	0.580	11.320
100 %	0.483	0.000	13.820
	0.508	0.016	13.820
	0.534	0.032	13.820
	0.560	0.047	13.820
	0.586	0.061	13.820
	0.613	0.075	13.820

ID 9807172B

%of heit	Mainsail x	Mainsail y	Mainsail z
0 %	0.046	0.000	1.320
	0.934	0.000	1.320
	1.822	0.000	1.320
	2.710	0.000	1.320
	3.598	0.000	1.320
	4.486	0.000	1.320
20 %	0.133	0.000	3.820
	0.891	0.190	3.820
	1.650	0.274	3.820
	2.411	0.274	3.820
	3.173	0.200	3.820
	Without Jib		
40 %	0.221	0.000	6.320
	0.837	0.231	6.320
	1.461	0.364	6.320
	2.091	0.417	6.320
	2.730	0.357	6.320
	3.373	0.236	6.320
60 %	0.308	0.000	8.820
	0.765	0.223	8.820
	1.231	0.370	8.820
	1.710	0.414	8.820
	2.199	0.370	8.820
	2.693	0.284	8.820
80 %	0.396	0.000	11.320
	0.656	0.138	11.320
	0.923	0.244	11.320
	1.199	0.297	11.320
	1.487	0.293	11.320
	1.780	0.261	11.320
100 %	0.483	0.000	13.820
	0.512	0.009	13.820
	0.540	0.018	13.820
	0.569	0.025	13.820
	0.599	0.031	13.820
	0.628	0.038	13.820

ID 96092335

%of heit	130%Jib x	130%Jib y	130%Jib z	Mainsail x	Mainsail y	Mainsail z
0 %	- 3.780	0.000	0.000	0.046	0.000	1.320
	- 2.812	0.136	0.000	0.934	0.000	1.320
	- 1.843	0.272	0.000	1.822	0.000	1.320
	- 0.875	0.408	0.000	2.710	0.000	1.320
	0.094	0.544	0.000	3.598	0.000	1.320
	1.062	0.681	0.000	4.486	0.000	1.320
20 %	- 2.998	0.000	2.140	0.133	0.000	3.820
	- 2.305	0.429	2.140	0.888	0.176	3.820
	- 1.568	0.667	2.140	1.645	0.322	3.820
	- 0.805	0.795	2.140	2.406	0.400	3.820
	- 0.027	0.861	2.140	3.173	0.363	3.820
	0.760	0.886	2.140	3.947	0.222	3.820
40 %	- 2.215	0.000	4.280	0.221	0.000	6.320
	- 1.771	0.442	4.280	0.834	0.227	6.320
	- 1.272	0.719	4.280	1.452	0.405	6.320
	- 0.723	0.850	4.280	2.081	0.483	6.320
	- 0.145	0.898	4.280	2.722	0.442	6.320
	0.448	0.898	4.280	3.371	0.331	6.320
60 %	- 1.433	0.000	6.420	0.308	0.000	8.820
	- 1.186	0.332	6.420	0.761	0.218	8.820
	- 0.893	0.570	6.420	1.222	0.389	8.820
	- 0.552	0.715	6.420	1.699	0.470	8.820
	- 0.176	0.790	6.420	2.191	0.462	8.820
	0.217	0.832	6.420	2.691	0.410	8.820
80 %	- 0.650	0.000	8.560	0.396	0.000	11.320
	- 0.541	0.172	8.560	0.651	0.144	11.320
	- 0.414	0.318	8.560	0.914	0.261	11.320
	- 0.255	0.419	8.560	1.190	0.330	11.320
	- 0.073	0.486	8.560	1.476	0.362	11.320
	0.122	0.535	8.560	1.768	0.374	11.320
100 %	0.132	0.000	10.700	0.483	0.000	13.820
	0.144	0.016	10.700	0.511	0.012	13.820
	0.159	0.030	10.700	0.538	0.023	13.820
	0.173	0.044	10.700	0.567	0.033	13.820
	0.189	0.056	10.700	0.595	0.042	13.820
	0.207	0.066	10.700	0.624	0.051	13.820

Table 2: Definition of sail geometry

4 Numerical Modeling

A comparison between real measurements and numerical predictions can only be valid if the geometries used for CFD simulation are identical to those in the reality. The surfaces generation from the net of points provided by Masuyama's et al. was carefully carried out in Rhinoceros and the grid generation process in ICEM-CFD. The reference data were in full scale so the numerical modeling was also made at the same scale. The sails were treated as rigid membranes.

In this paper only the best results are going to be presented. During the geometry generation process different mistakes were made and it was discovered the importance of precision. A couple of degrees in heel or apparent wind angle resulted in significant discrepancies between calculated and real values and so the geometry process took a lot of time to make sure the simulations were identical to full scale data. In the same way, the treatment of the surface in Rhino was very important for the later meshing. It must be also emphasised that more than five meshes were tested for each geometry trying to find out the best parameters and the optimal number of elements according to the capacity of the computer. With the suitable meshes

different parameters of the numerical scheme and the boundary conditions were tested to obtain the best combination among them. Therefore, the real number of studied cases was huge even if in this article only the most satisfactory results are presented.

The calculations were run using ANSYS CFX-10 with two independent CPU Pentium IV 3.2 GHz computer with 3GB of RAM. For a mesh size of 1,300,000 elements the typical CPU time for achieving the specified convergence was around11 h.

4.1 Domain and Mesh

The extension of the computational domain was 100 m upstream, 120 m downstream, 60 m upwards, and 60 m on each side. On the configuration jib + mainsail (ID 96092335), the extension downstream was 140 m. These domains were considered to be sufficient for a good development of the flow without creating wall effects. The grid was structured and concentrated next to the sails.

The sails were generated as surfaces with no thickness, on which "no-slip" boundary condition was applied. The variable that CFX uses to check the location of the first node of the mesh away form a wall is called Yplus (y^+). It is the dimensionless distance from the wall and it is based on the distance from the wall to the first node and the wall shear stress, as seen in equation [3]. This value permits evaluating the quality of the mesh next to walls and its capability of detecting the boundary layer. The size of the elements in the direction normal to the sail was around 1-3 mm and it was adjusted to $y^+ = 1 - 90$ which is a range similar to the ones used in [14], [15], [16], [17] and to the recommended value in the CFX documentation [18].

$$y^+ = \frac{\nabla y \cdot u_\tau}{\nu} \qquad \text{Equation [3]}$$

The "determinant 2x2x2" criterion was used to verify the quality of the meshes. A determinant value of 1 would indicate a perfectly regular mesh element, 0 would indicate an element degenerated in one or more edges, and negative values would indicate inverted elements. It was tried to get determinants higher than 0.6 for all the hexahedrons of the meshes.

The number of hexahedrons was around $1.3 \cdot 10^6$ for the configurations of mainsail alone and $2.1 \cdot 10^6$ for jib + mainsail. The bottom surface of computational grid was taken at the deck plane of the boat (z = 0 m) when considering mainsail alone and z = - 1.5 m with jib + mainsail configuration.

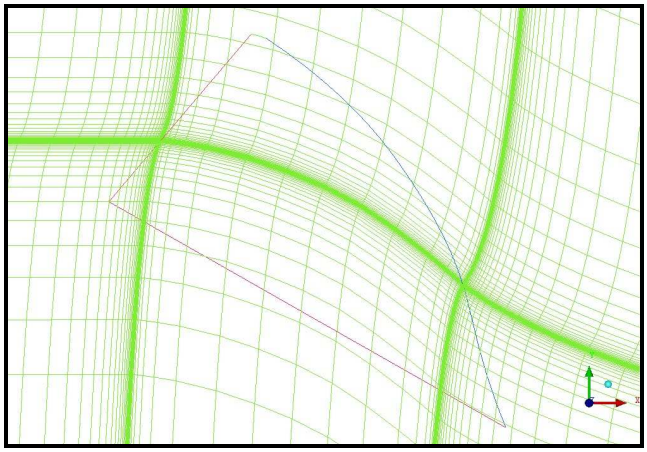

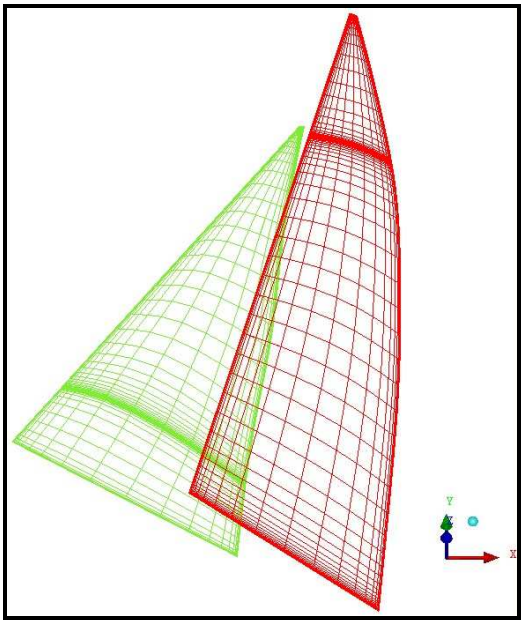

Figure 2 and Figure 3: Details of the meshes

4.2 Boundary Conditions

It has been tried to impose the most suitable boundary conditions necessaries to reproduce the real behaviour of the Fujin.

- Inlet: The speed normal to the inlet surface was set constant and different in each case. The wind gradient was not taken into account for the numerical calculation because it was seen in Masuyama et al. (2007) that it was not so significant. This means that the apparent wind angle and speed were assumed to be constant in the vertical direction. Turbulence intensity was set at 2% (low) and length scale of turbulence of 0.5 m (1/10L) according to the recommendations in the CFX documentation [18].
- Outlet: the averaged pressure over the surface was set to zero.
- Walls: the condition imposed was "free-slip".
- Floor (Deck): The boundary condition was "free-slip". Some tests were studied with "no-slip" condition on the bottom and there was not a significant variation in the result so it was decided to use "free-slip" because it required less time.
- Sails: as mentioned before, the "no-slip" condition was set.

4.3 Numerical Scheme

As usual, in order to close the RANS equations and determine the Reynolds stresses a turbulence model was required. The model chosen was the SST (Shear Stress Transport) as in [8], [15] and [16]. This model was developed in 1994 by Menter. The SST accounts for the transport of the turbulent shear stress and gives highly accurate predictions of the onset and the amount of flow separation under adverse pressure gradients. The SST is one of the most popular turbulence models in external aerodynamics and it is used widely in the industry. The reason for the wide spread usage of this model in aeronautics is that it is robust; it allows an integration through the viscous sublayer without much computational effort and has advanced separation prediction capabilities, [19].

In order to judge convergence the value of the RMS (root mean square) residual was considered. The condition imposed was 10^{-5}. According to the CFX documentation [18] reaching this value implies a "good convergence". It was tried a RMS target of 10^{-6} but the CPU time needed far exceeded 24 hours and it was considered excessive.

The Reynolds number of the simulations was around $2.3 \cdot 10^6$ with a characteristic length of 5 m. The timestep, with the same length, was set to be "small" and obtained with eq. [4] as suggested in the CFX modeling documentation [18]. The values were 0.172 s, 0.174 s and 0.184 s for the first, second and third case respectively.

$$timestep = \frac{1}{4}\frac{L_c}{V} \qquad \text{Equation [4]}$$

In the third case, jib + mainsail configuration, the timestep corresponding to the eq. [4] was too small, the convergence was difficult to achieve and the periodicity of the phenomena was captured. The three cases were studied from a steady state point of view so in this third case the timestep was increased to avoid the periodic fluctuations, and finally the timestep in this case was set to 4 s.

5 Results

One of the advantages of these commercial codes is that they give a great amount of outputs. In this article it has paid attention to the values which were useful to understand better the phenomena involved and the ones for comparing with the data of the reference paper. As it can be seen in table 3, the lift and drag

coefficients has been obtained as well as the position of the center of effort in each case. In the same table the reference data have been included in order to facilitate the comparison.

	Reference study	Present study(CFD)
ID 9807172F		
C_L	1.222	1.164
C_D	0.371	0.326
X_{CE} (m)	1.552	1.550
Z_{CE} (m)	5.686	4.810
ID 9807172B		
C_L	1.266	1.083
C_D	0.502	0.456
X_{CE} (m)	1.660	1.510
Z_{CE} (m)	5.834	5.910
ID 96092335		
C_L	1.418	1.497
C_D	0.260	0.344
X_{CE} (m)	0.433	0.280
Z_{CE} (m)	4.138	4.570

Table 3: Comparison of results

The results of the first two cases (main sail alone) are highly satisfactory. The eight values differ less than 16% and five of them less than 10%. It can also be observed that the values of the present study are generally lower than the ones obtained in the Fujin. It must be again emphasize that the data provided in the paper of Masuyama et al. [11] included the influence of the mast in the results.

Because of the fact that there was no information about the geometry of the mast some test with supposed masts were carried out in the first two cases. In all the studied tests the results of both C_D and C_L improved considerably to even differences below 5%. Three masts were defined according to the images of the boat that are included in the reference paper. One of the masts had an elliptic section and that section was constant along the height of the mast (see figure 4). The second had also an elliptic form but it was decreasing its shape from bottom to top. The third mast had a circular section. The best results were obtained with the elliptic and constant mast for which more than four meshes were tried. For example for the first case (ID 9807172F) the coefficients obtained were 0.381 in drag and 1.258 in lift. This supposes differences of 2.60 % and 2.98 % respectively for a mast with an elliptic and constant section.

It must also be considered that the geometry of the hull was not included in the simulations neither the rigs. Although the calculus would be enormous, including the hull and the rig would make the drag coefficient be closer to real values and presumably, the lift coefficient would have the same trend. It must be highlighted that meshing one sail is complicated and doing it for sail and mast much more. The difficulty arises from the fact that the sail has no thickness but the mast does. It is very laborious to make a structured mesh next to the sail plus mast and control all the parameters without increasing the number of elements excessively.

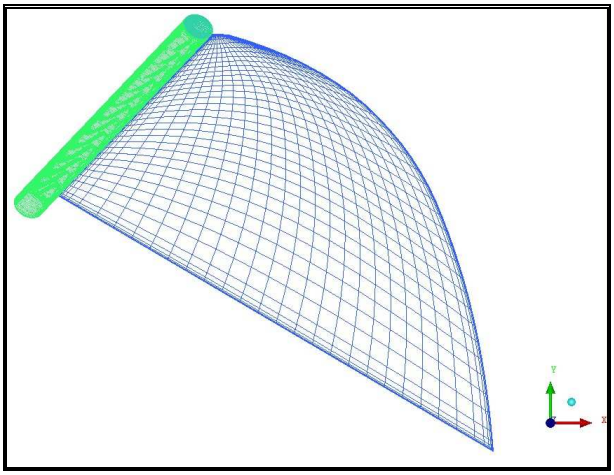

Figure 4: ID 9807172F with mast

With reference to the position of the center of effort in the first two cases the trend is uncertain. In the first case (ID 9807172F), X_{CE} is similar in the two columns but the Z_{CE} in the present study is lower than the reference value. On the other hand, in ID 9807172F it happens the opposite. Z_{CE} is almost equal as the longitudinal position in the present study is lower than of the reference. Anyway, the differences are 15% at the most so they can be judged satisfying, taking into account that the full geometry was not included in the simulations.

The results obtained in the third case, jib + mainsail configuration (ID 96092335), are less optimistic; especially the longitudinal position of the center of efforts and the drag coefficient. These errors may be due to the quality of the mesh. There may be needed more elements to capture all the phenomena involved especially between and behind the sails. Another reason, and not just in the third case, can be that the measured moments in the Fujin contained a large amount of moment resulted from the mass of the dynamometer frame and rigging. This moment should have been subtracted from the measured ones using the heel angle. If there was a slight error in the position of the center of gravity of the dynamometer frame or in the measured heel angle, the error in the calculated moments would have become considerably large.

On the other hand both the vertical position of the center of efforts and the lift coefficient differ only 10% and 6% respectively in this third case. With this configuration the program enables to calculate separately the lift and drag coefficients: mainsail (C_D= 0.439 and C_L= 1.195) and jib (C_D= 0.222 and C_L= 1.881). As it can be observed the jib gives a much effective thrust. The fore sail, with less area, produces more lift and less drag than mainsail does. It is thought that it occurs because the circulations of main and jib tend to oppose and cancel each other in the area between the two sails and therefore more air is forced over leeward side of the jib, [14].

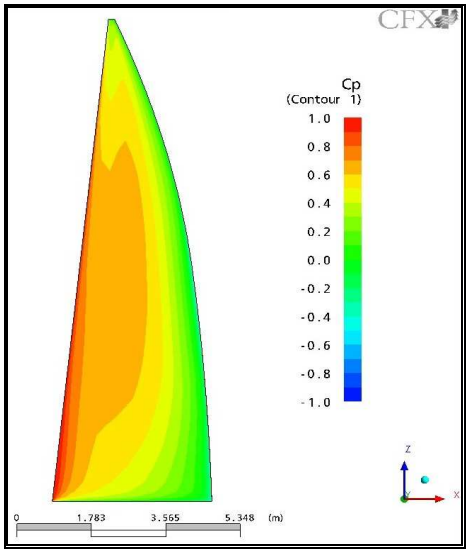

Windward side

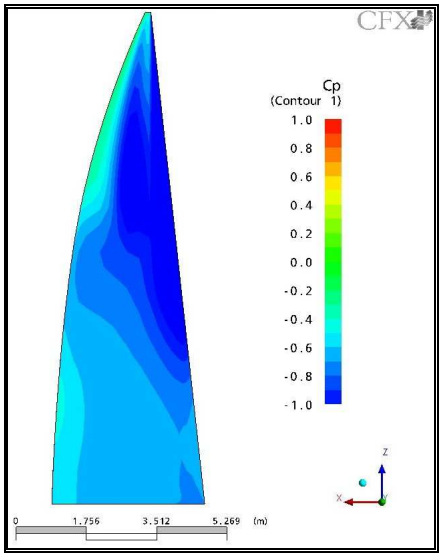

Leeward side

Figure 5: Pressure coefficient, ID 9807172F

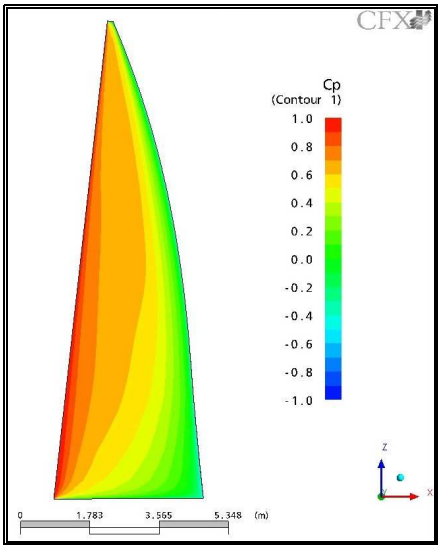

Windward side

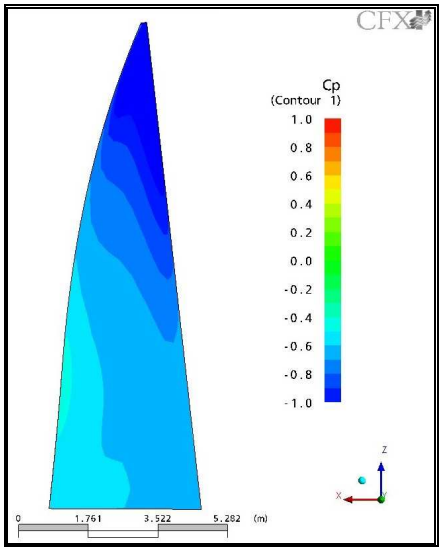

Leeward side

Figure 6: Pressure coefficient, ID 9807172B

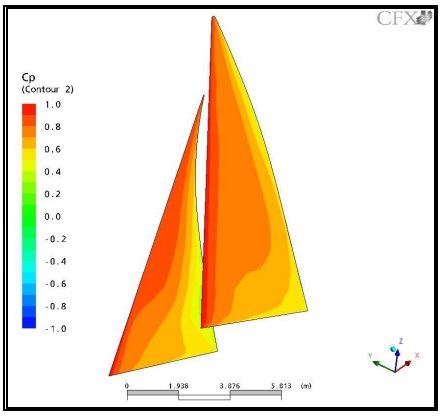

Windward side

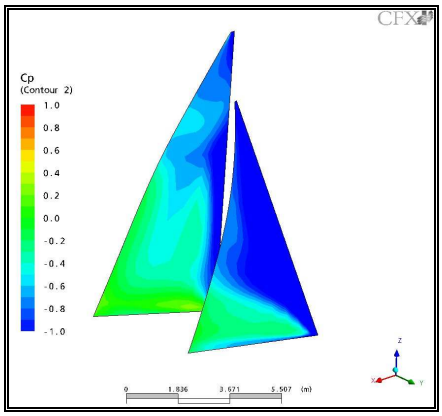

Leeward side

Figure 7: Pressure coefficient, ID 96092335

In figures 5, 6 y 7 the pressure coefficient for each case can be seen. The images have been compared with the numerical results of Masuyama et al. [11] and they are similar. The pictures of pressure coefficient of the reference paper are not included in this document because of their bad quality. As when comparing values, the distribution of pressure coefficient is better in the first two cases than in the third. In this last case the only part that can be judged satisfactory is the leeward side of the jib. It can be due to the detachment of the flow on that side which affect considerably the performance of the mainsail. In this situation the program is not able to capture the vortices on the leeward side of the mainsail. It would be needed a better mesh and a transient study.

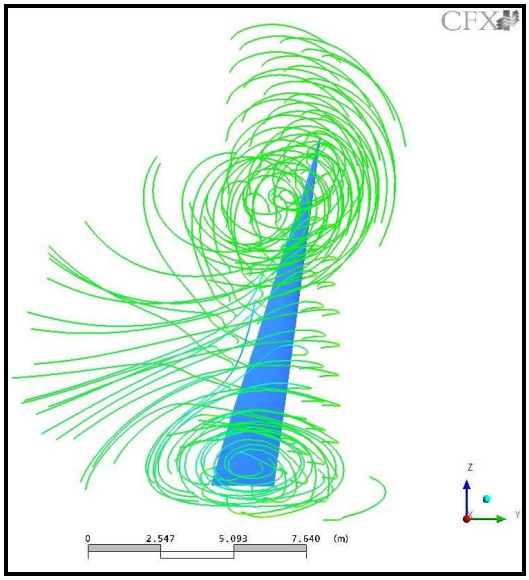

Figure 8 : Two vortices of ID 9807172B

In figures 8 and 9 it can be observed one of the most interesting phenomenon involved in the interaction between air and the sails which is the appearance of vortices. In figure 8, two vortices can be seen: one on the top of the sail and the other at the bottom. Just as it was expected the second vortex is gotten flat and in a higher height than the boom. The presence of the deck (floor) tends to tangle up the two tip vortices and affect the flow up to the middle of the mast, usually, increasing both lift and drag. In figure 9 the streamlines and air velocity around the main sail in a plane at 50% of its height are presented. The pink line represents the intersection of the sail with the plane. There is separation of the flow and a vortex at the trailing edge. Even if it is usually considered that when upwind there is no separation and potential methods are used, it is demonstrated that there is detachment of the flow. Because of this fact, viscous CFD codes must be use as the one in this work.

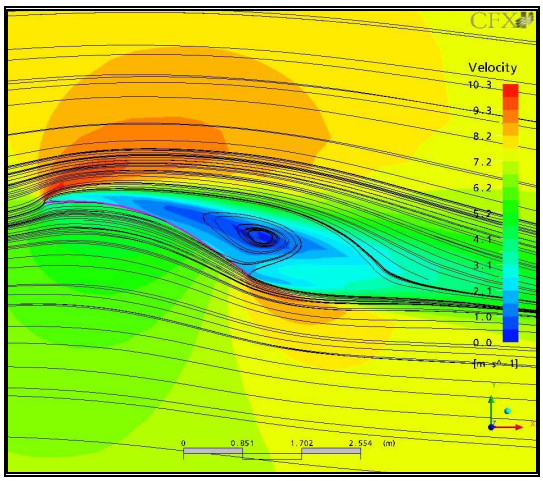

Figure 9 : Plane at half the luff of mainsail ID 9807172F

6 Conclusions

The present work aimed at developing a methodology for studying racing yacht sails in upwind conditions by combining full scale measurements with 3D RANS simulations. These viscous solvers have now reached a mature stage and can be used as top-quality design tools to study sail flow and to perform optimization of modern rigs. Not only full scale force predictions can be achieved, but the whole flow field around the sails can be studied for a better understanding of the main flow features. For example, the detachment of the flow in upwind condition that has been showed in this document suggests that viscous CFD codes must be used and not potential codes as it is usually done.

Large amount of tests were carried out before obtaining the results that are included in this document. A positive agreement of the present numerical study with the reference one is considered, both in terms of qualitative aspect and in terms of numerical values. With this work we have demonstrated that our research group is in more than a respectable position in the field of the CFDs. Furthermore, we have tried to include all the necessary input data for the reader to be able to reproduce the simulations and the outputs to compare, since it is very unusual to have access to this information.

It is noteworthy the significance positioning the deck level when simulating sail flow in upwind conditions. The deck has a strong influence on the tip vortices generated at the sail's foot. Modeling the boom, the deck, spreads, etc. could as well increase the accuracy of the simulation, but at the cost of an even more complex mesh. The study was carried out without mast. Nevertheless, the analyzed cases with supposed masts demonstrate the positive influence in the trend of the results to the real values.

A CFD code is a cost-effective tool for the performance prediction of a sailing yacht. If experimental results can be accurately reproduced using the same methodology for a fair number of cases, the latter can be afterwards trusted for providing reliable results for new cases, for which no experimental data are available [16]. The study shows that CFD codes can be used with remarkable accuracy.

7 Acknowledgements

This paper is framed within the work that the first author is realising in the CEHINAV research group thanks to a scholarship of the Polytechnic University of Madrid of the program for the researchers in formation for the accomplishment of the doctorate in its departments and institutes.

References

[1] W.C. Lasher, *On the Application of RANS Simulation for Downwind Sail Aerodynamics*, in: 14th Chesapeake Sailing Yacht Symposium, Annapolis, Maryland, USA, 1999.

[2] S. Shankaran, T. Doyle, M. Gerritsen, G. Iaccarino, A. Jameson, *Improving the Design of Sails using CFD and Optimization Algorithms*, in: 1st High Performance Yacht Design Conference, Auckland, New Zealand, 2002.

[3] S.J. Collie, P.S. Jackson, M. Gerritsen, *Validation of CFD Methods for Downwind Sail Design*, in: 1st High Performance Yacht Design Conference, Auckland, New Zealand, 2002.

[4] S.J. Collie, P.S. Jackson, M. Gerritsen, J.B. Fallow, Two Dimensional CFD Based Parametric Analysis of Downwind Sail Designs, RINA, 2004.

[5] M. Caponnetto, A. Castelli, P. Dupont, B. Bonjour, P.L. Mathey, S. Sanchi, M.L.Sawley, *Sailing Yacht Design Using Advanced Numerical Flow Techniques*, in: 14th Chesapeake Sailing Yacht Symposium, Annapolis, Maryland, USA, 1999.

[6] P. Jones, R. Korpus, *International America's Cup Class Yacht Design Using Viscous Flow CFD*, in: 15th Chesapeake Sailing Yacht Symposium, Annapolis, Maryland, USA, 2001.

[7] H.J. Richter, K.C. Horrigan, J.B. Braun, *Computational Fluid Dynamics for Downwind Sails*, in: 16th Chesapeake Sailing Yacht Symposium, Annapolis, Maryland, USA, 2003.

[8] G. Clauss, W. Heisen, *CFD Analysis on the Flying Shape of Modern Yacht Sails*, in: 12th International Congress of the International Maritime Association of the Mediterranean, Lisbon, Portugal, 2005.

[9] J. H. Milgram, D. B. Peters, N. Eckhouse, *Modelling IACC Sail Forces by Combining Measurements with CFD*, in: 11th Chesapeake Sailing Yacht Symposium, Annapolis, Maryland, USA, 1993.

[10] Y. Masuyama, T. Fukasawa, *Full Scale Measurement of Sail Force and Validation of Numerical Calculation Method*, in: 13th Chesapeake Sailing Yacht Symposium, Annapolis, Maryland, USA, 1997.

[11] Y. Masuyama, Y. Tahara, T. Fukasawa, N. Maeda, *Database of Sail Shapes vs. Sail Performance and Validation of Numerical Calculation for Upwind Condition*, in: 18th Chesapeake Sailing Yacht Symposium, Annapolis, Maryland, USA, 2007.

[12] H. Brandt, K. Hochkirch, *Entwicklung einer meßyacht zur analyse der segelleistung im orginalmaßstab (Design and Construction of a full scale Measurement System for the Analysis of Sailing Performance)*, Tech. rep., Technische Universität Berlin, 2000.

[13] H. Hansen, P.S. Jackson, K. Hochkirch, *Comparison of Wind Tunnel and Full-Scale Aerodynamic Sail Force Measurements*, in: 1st High Performance Yacht Design Conference, Auckland, New Zealand, 2002.

[14] J. Yoo, H.T. Kim, Computational and Experimental Study on Performance of Sails of a Yacht, Ocean Engineering, number 33, pages 1322–1342, 2006.

[15] A.B.G. Quérard, P.A. Wilson, *Aerodynamic of Modern Square Head Sails: a Comparative Study between Wind Tunnel Experiments and RANS Simulations*, International Journal of Small Craft Technology, number 147, 2007.

[16] C. Ciortan, C. Guedes-Soares, *Computational Study of Sail Performance in Upwind Condition*, Ocean Engineering, number 34, pages 2198-2206, 2007.

[17] W.C. Lasher, J.R. Sonnenmeier, *An Analysis of Practical RANS Simulations for Spinnaker Aerodynamics*, Journal of Wind Engineering and Industrial Aerodynamics, number 96, pages 143-165, 2008.

[18] ANSYS, ANSYS CFX-Solver, Release 10.0: Modelling.

[19] F. Menter, Y. Egorov, *Turbulence Modeling of Aerodynamic flows*, in: International Aerospace CFD Conference, Paris, France, 2007.